

3.0 MATHEMATICAL MODEL

The internal manifolded solar collector was described in Chapter 1. When several such collectors are connected in parallel, the basic configuration remains the same, that is the resulting hydraulic pipe network comprises an upper and lower manifolds with risers in parallel. In the following the conceptual model of such a pipe network will be discussed and subsequently the model for the solar collector will be developed. The model proposed here is quite different from those available in the literature and will be discussed in details.

When several collector modules are connected in parallel, the flow rates in the risers are never equal. The basic aim of the present work is to study flow distribution in collector array and suggest methods to maintain flow in each riser nearly equal such that the collector array efficiency can be maintained same as that of a single collector module. Theoretically, the simplest method to obtain the same flow rate in each riser is to keep the pressure in the manifold constant throughout its length. This implies a very large manifold with negligible pressure variation across the manifold.

A simple method is to have a manifold such that the

cross-sectional area decreases at a rate that keeps the fluid velocity nearly constant while the mass flow rate decreases. This method has the disadvantage that while it works for a particular flow rate, it will not for another flow rate. Further, this technique is certainly not practical for solar collector since tapered manifold has to be designed for a particular number of collectors in parallel and an inventory of collectors are to be kept.

It would be sufficient to develop a method such that the flow in risers are practically equal or the flow distribution is such that the collector array efficiency is not reduced by a certain percentage, for example one percent. Thus the methodology developed here is for collector having same size of manifolds with constant diameter.

It would be worthwhile to discuss the behaviour of manifold both for dividing and combining flow separately to understand the pressure variations in the manifolds. Basically, the pressure change in a manifold having side port (tee junction) is caused by wall friction in the section between the ports and due to momentum change at the port. In a dividing manifold when the fluid leaves the side port, the pressure at the port rises because an opposing force is needed to cause the exit fluid to lose some of its forward momentum as it leaves. Similarly, a pressure change occurs at the side port of a combining manifold as the entering fluid acquires momentum.

In a dividing manifold having several side ports the pressure in the manifold continues to rise and fall. For an isolated dividing manifold, the total pressure will continue to fall while the static pressure rises. When the static pressure rise due to momentum change at the side ports outweighs the static pressure drop due to wall friction in the section between the ports, for a uniform port discharge pressure, the flow leaving the port is not the same and exhibits increasing flow towards the closed end [Collier (1976)].

The flow distribution will strongly depend upon the wall friction and the ratio of the fluid pressure to the specific kinetic energy at the entrance. For no wall friction the flow continuously increases and the last port will have the maximum flow. The wall friction affects the manifold pressure and thus the flow distribution. Thus as the wall friction increases a stage is reached when the flow starts decreasing to a minimum before rising to the last port. For an isolated dividing manifold, it is possible to design the manifold diameter in such a way such that the flow leaving the side ports are practically the same for a given value of ratio of fluid pressure to the specific kinetic energy at the entrance. In general, keeping the manifold diameter large reduces the manifold velocity and the said ratio, thereby improving the flow distribution [Acrivos(1950)].

In case of combining manifold where the fluid enters the manifold from a constant pressure source, the wall friction and the

momentum effect act in the same direction, causing the pressure in the manifold to become smaller in the direction of flow, that is towards the open end of the manifold where the total fluid leaves. In other words, the total pressure and the static pressure fall towards the header outlet. The static pressure difference across the port(tee junction) due to momentum changes reinforces the head loss due to wall friction. The flow is always the maximum in the port near the exit. In such a manifold the flow variation is much more than in the case of dividing manifold. Thus, a larger combining manifold is needed for the same flow variation in a dividing manifold [Acrivos(1950)].

In a solar collector the dividing and combining manifolds are connected by the parallel risers of diameter smaller than that of manifold. The pressure variation in the manifolds are similar as described above except that the risers connecting the manifolds alter the flow distributions since the ports are no longer in communication with constant pressure. In the riser the pressure changes are due to wall friction and also at the ports at either ends due to flow direction and area change. The pressure variations in the manifolds are now interdependent.

It can be visualised that the flow distribution in an array of solar collector in parallel cannot be uniform unless it is designed so. In the following a mathematical model is developed which describes the interaction of the manifolds and riser. The assumptions made in the model are mentioned as the sub-components

are described. However, the general assumptions are as follows :

1. The model is for isothermal fluid flow i.e. the temperature effect on the fluid properties is neglected.
2. The thermosiphon effect, that is the head developed due to density difference in the parallel risers is neglected.
3. The flow is steady.
4. The effect of non-uniform velocity in the manifolds or tee junction is accounted for in the semi-empirical loss coefficients.
5. The interaction of adjacent tees on the loss coefficient is negligible and is neglected.
6. Flow in the manifold and riser is Reynolds number dependent.

The internal manifolded solar collector array can be visualised as a pipe network consisting of two manifolds and parallel risers (Fig. 1b). It is, therefore, possible to apply the hydraulic network algorithms developed by Daniel (1966), Bending and Hutchinson (1973) or the diakoptics method of Gay and Middleton (1971). In all these algorithms, the pressure changes considered are due to pipe friction only, neglecting losses at tees, bends etc,

as the later would be negligible in the types of network for which the algorithms were developed. On the other hand, in case of a solar collector there are two tee junctions for every riser. Further, there is a cross-sectional area change at such tee junction, since the manifold is always sized greater than the riser.

In the present work such changes are accounted for as described in Sec.3.1. The approach is slightly different employing the loss coefficients as defined by Miller (1978) rather than the momentum loss coefficients for the tee junction. The former is well documented as a function of the tee geometry and flow ratios. On the other hand, only few measurements are available in the literature for the momentum coefficients.

The model derived below is discrete in nature as briefly discussed above, unlike the continuous model developed by Bajura and Jones(1976), Pigford et.al.(1983) and McPhedran et.al.(1983). Thus the present model will not be restricted to large number of risers.

The flow at tee junctions is described in detail in Sec. 3.1. Sec. 3.2 gives the frictional loss in riser and manifold. The network equations, selection of the algorithm, accounting of flow reversals and the effect of temperature are described in Sec. 3.3 to 3.8. Sec. 3.9 describes the estimation of collector array efficiency due to maldistribution.

3.1 Flow at Tee Junction

The pressure changes at a tee junction, both for dividing and combining flow, can be treated either by momentum or energy conservation. Acrivos et. al (1959), Bajura and Jones (1960), McFhedran (1983) and Pigford (1983) employed momentum coefficients for describing flow at a tee junction. Bajura and Jones (1976) advocated the use of momentum conservation rather than energy conservation on the basis that it is very difficult to allow properly for localised heating effects around the junction as mechanical energy is lost through viscous dissipation. Momentum coefficients are, however, not widely reported in the literature (Pigford (1983)).

All the previous authors had employed constant values of momentum coefficients and they were assumed to be independent of tee geometry and flow ratio (riser flow to manifold total flow). In a solar collector the flow ratio changes at each tee junction (riser-manifold), typically 0.1 to 1.0, depending upon flow distribution. Also the area ratio of riser to manifold cross-sectional areas will affect the loss coefficients. The variation in the coefficients can be appreciated from limited data obtained by Pigford (1983). The momentum coefficients varied from 0.26 to 0.49 in the dividing manifold, while it varied from 0.91 to 2.41 in the combining fold. This variation is certainly significant.

The only well documented data for tee loss coefficients which account for both the tee geometry and flow ratio are that of Miller (1978). The coefficients are semi empirical and are based on energy conservation. These coefficients are used in the present model and discussed in detail below.

Fig. 3.1 shows the flow at a tee junction and the numbering nomenclature. The convention adopted is that the leg carrying the total flow is called leg 3. The branch leg of the tee junction is called leg 1 and the leg carrying throughflow is called leg 2.

The loss coefficients K_{ij} shown in Fig. 3.1 are defined as :

$$K_{ij} = \frac{\text{total pressure in leg } i - \text{total pressure in leg } j}{\text{mean velocity pressure in leg } 3} \quad \dots(3.1)$$

The flow ratio is always expressed as Q_1/Q_3

3.1.1 Dividing Tee Junction

Considering flow entering the branch of a 90° sharp edged tee, Fig. 3.2, with $A_1/A_3 = 1$. For very small flows into the branch the static pressure in leg 3, and the velocity pressure in the branch is virtually zero. Since the energy level in the branch

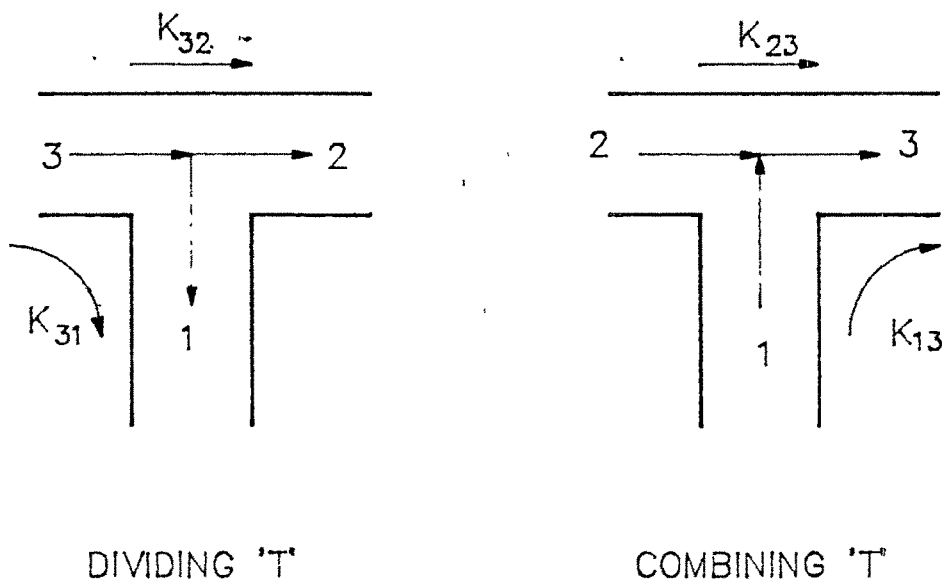


Fig. 3.1 Flow at Tee Junction and Numbering Nomenclature

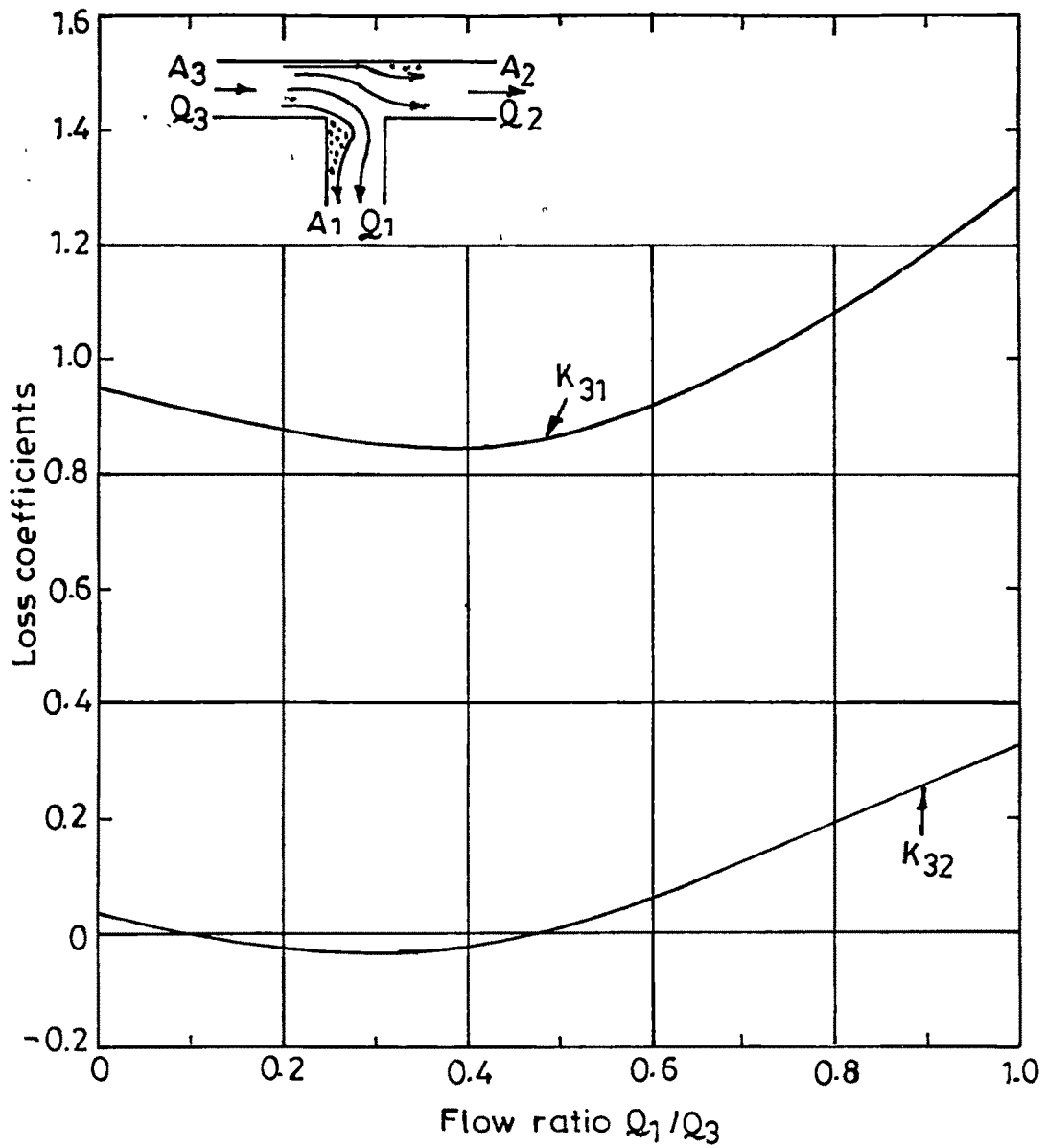


Fig. 3.2 Loss coefficients for sharp edged 90° dividing 'T.'

is lower by the velocity pressure in the leg 3, the branch loss coefficient is positive at about $K_{31} = 1$. At the other extreme, when all the flow is into the branch [$Q_1/Q_3=1$] the loss coefficient is similar to that of a mitre bend at about 1.1. In between the two extremes the coefficient drops to a minimum of about 0.85 at $Q_1/Q_3 = 0.40$.

The loss coefficient for the throughflow K_{32} is virtually zero until $Q_1/Q_3 = 0.50$. For low flow ratios the fluid drawn off by the branch consists of the slow moving fluid close to the walls, so the energy per unit mass of the fluid in the throughflow may increase slightly. This increase is to some extent balanced by the diffusion loss as the throughflow slows down at the tee junction. Above $Q_1/Q_3 = 0.5$ the throughflow coefficient K_{32} increases steadily upto 0.35 when all the flow is into the branch. K_{32} is not greatly affected by changes in the area ratio A_1/A_3 . Reducing the area ratio increases branch loss coefficient K_{31} , but the pressure loss in a branch is a smaller percentage of the branch velocity pressure.

Viewed from the momentum conservation approach the throughflow coefficient is the pressure recovery coefficient considered by Acrivos (1959) and Pigford (1983). The pressure rise at a dividing tee junction can be appreciated from the momentum balance at the tee, e.g. see Acrivos (1959) or Pigford (1983). The effect termed as the Bernoulli effect by McPhedran (1983), is important to account for in the total model since it influences the flow distribution. It is accounted for in the present work by the loss coefficient K_{31} .

The loss coefficients as a function of flow ratio Q_1/Q_3 and area ratio A_1/A_3 are given by Miller (1978). The effect of ratio of radius at branch-main leg junction to the branch diameter is also included. For the purpose of design and computer simulation it is more convenient to use the correlation given by Gardel (1955) presented by Collier (1976). These are as follows :

$$\begin{aligned}
 K_{31} = & - 0.95(1-q)^2 \\
 & - q^2 [(1.3\cot(180-\theta)/2 - 0.3 + (0.4-0.1a)/a^2)(1-0.9(r/a)^{1/2})] \\
 & - 0.4q(1-q) (1+1/a)\cot(180-\theta)/2
 \end{aligned}
 \tag{3.2}$$

$$K_{32} = - 0.03(1-q)^2 - 0.35q^2 - 0.2q(1-q)
 \tag{3.3}$$

where q = flow ratio, Q_1/Q_3

a = area ratio, A_1/A_3

r = ratio of radius at branch to main junction to the
branch diameter

θ = angle of junction, 90° in the present case.

3.1.2 Combining Tee Junction

Fig. 3.3 gives the loss coefficients for a combining sharp

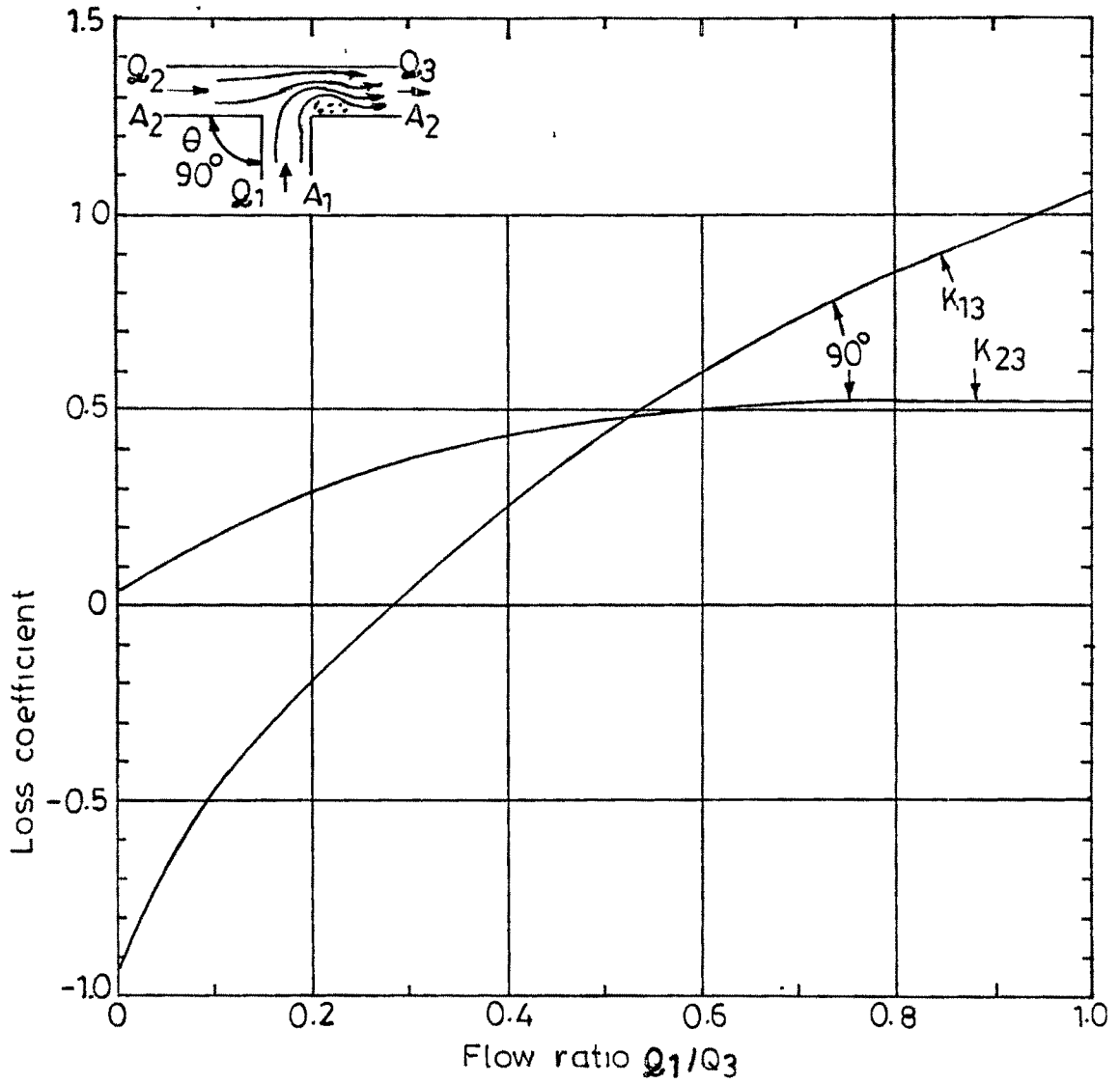


Fig. 3.3 Loss coefficients for sharp edged 90° combining 'T'.

edged 90° tee, area ratio $A_1/A_3 = 1$, as a function of flow ratio Q_1/Q_3 .

Consider first flow entering from branch leg 1 into leg 3. For zero branch flow the pressure in the branch is essentially the static pressure of the throughflow. If the pressure in the branch is raised slightly, a small flow will leave the branch and be accelerated upto the velocity in leg 3. There is a transfer of energy from the throughflow (leg 2) to the flow from the branch, so the loss coefficient for the branch is negative. When the flow ratio is close to zero the branch loss coefficient K_{13} is -1.0. The corresponding throughflow coefficient K_{23} is positive at about 0.05. As the flow ratio increases the branch loss coefficient K_{13} becomes positive at a flow ratio of 0.3, reaching a maximum at about 1.1 when all the flow is from the branch. The corresponding value of K_{23} increases steadily from near zero upto a maximum of about 0.55 when all the flow is entering from the branch.

If the area ratio A_1/A_3 is less than unity the velocity pressure in the branch, for a given Q_1/Q_3 , is greater and the branch loss coefficients are higher. For instance, with all the flow from the branch, the branch loss coefficient will be greater than the the coefficient with equal area by roughly the increase of the square of the area ratio. Variation in the area ratio has a small effect on the throughflow coefficient K_{23} .

Gardel's tee loss coefficients for combining flow are as follows :

$$\begin{aligned}
 K_{13} = & - 0.92(1-q)^2 \\
 & - q^2[(1.2-r^{1/2})(\cos(\theta/a)-1) + 0.8(1-1/a^2) - (1-a)\cos(\theta/a)] \\
 & + (2-a)q(1-q)
 \end{aligned}
 \tag{3.4}$$

$$\begin{aligned}
 K_{23} = & 0.03(1-q)^2 \\
 & - q^2[1 + (1.62-r^{1/2})(\cos(\theta/a)-1) - 0.38(1-a)] \\
 & + (2-a)q(1-q)
 \end{aligned}
 \tag{3.5}$$

3.1.3 Applicability of the tee loss coefficients for solar collector network

Effect of spacing

The loss coefficients at dividing and combining tees given in the previous sections are for an isolated tee. In a solar collector, there will be several tee junctions spaced at certain intervals. According to Miller (1978), when the tees are spaced at 3 manifold diameters apart, or 4 branch diameters apart if the branch flow is less than 10 % of the total flow, the isolated tee loss coefficients can be used. Similar observations were made by

Acrivos (1959) and Pigford (1983) based on the experimental values.

The present day solar collector typically employ riser spacing of 100 - 125 mm which is about 4 - 5 manifold diameter (25 mm NB) or 10 to 12 branch diameters (9 mm). The isolated loss coefficients therefore can be used for a solar collector.

Effect of Reynolds Number

The tee loss coefficients given in Secs. 3.1.1 and 3.1.2 due to Gardell (1959) or Miller (1978) are for high Reynolds number (100,000). The flow in a solar collector is not highly turbulent and laminar flow in the risers are not unusual.

Miller (1978) recommended correction factors for lower Reynolds number for bends. However, for sharp bends, the effect of Reynolds number is not predominant. Fig. 3.4 reproduced from Fig. 5.82 of Miller (1978) indicates independence of Reynold number in the range of 800 - 100,000. Further, according to Perry (1963), the tee loss coefficient in the range of 500 - 1000, both for throughflow and branch loss coefficients, are not affected significantly by Reynolds number. Below $Re = 500$ the coefficient rises sharply with Reynolds number. The values are shown in Table 3.1. For comparison the coefficients for 90° elbow and different types of valves are also given. It is observed that for these fittings the loss coefficient is insensitive to Reynolds number in the range of 500 - 1000.

It is apparent that Miller's or Gardel's tee loss coefficients can be used upto $Re = 500$ without significant error. This indeed will be the case as shown in Chapter 6.

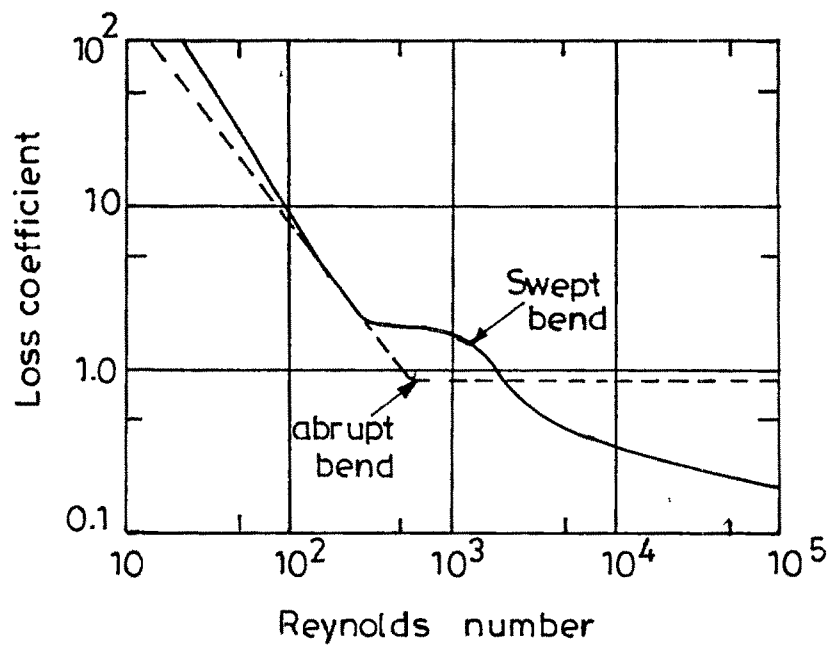


Fig.3.4 Effect of Reynold number on loss coefficient for sharp bend

Table 3.1 Loss Coefficients for Tee, Elbow and Valves in laminar
flow

Type of fitting	Loss coefficient, K (no. of velocity heads)			
	Reynolds No.			
	1000	500	100	50
a. Tee				
-standard along run (throughflow)	0.40	0.50	2.5	--
-branch	1.50	1.80	4.9	9.3
b. 90° elbow, short radius	0.90	1.00	7.5	16.0
c. Gate valve	1.20	1.70	9.9	24.0
d. Angle valve	8.00	8.50	11.0	19.0
e. Globe valve, disc plug	11.00	12.00	20.0	30.0

Source: Perry (1963), Table 5.20 after Kitteridge.

3.2 Friction flow in riser and manifold

The flow in a riser of a solar collector is normally laminar. The pressure change in a riser is due to friction because of viscous dissipation. The flow in a manifold can vary from laminar to turbulent.

The friction factor for laminar flow is given by

$$f = 64/Re \quad (3.6)$$

For turbulent flow, the friction factor is given by the explicit expression due to Swamee and Jain (1976)

$$f = \frac{0.25}{[\log(k/3.7D) + 5.74/Re^{0.9}]^2} \quad (3.7)$$

where, k is the pipe roughness, m .

3.3 Solar collector Network Model

Model, both for symmetric (U-manifolded) and asymmetric (Z-manifolded) configuration, will be derived. The pressure changes at tees, riser and manifold were discussed in Sec. 3.2 where the loss coefficients and friction factors were defined.

3.3.1 Network Pressure Equation

The pressure change in general is described as

$$\Delta P = K \cdot d U^2/2 \quad (3.8)$$

where, ΔP = pressure change, $N m^{-2}$

d = density, $kg m^{-3}$

U = velocity, $m s^{-1}$

K = loss coefficient, dimensionless

In a network, flow rates are normally employed as this variable is used to satisfy Kirchoff's law at each tee junction and during iteration. The pressure equation is then modified to

$$\Delta P = K \cdot d Q^2/2A^2 \quad (3.9)$$

where, A = cross-sectional area, m^2

Q = flow rate, $m^3 s^{-1}$

In fact this form is useful also since the tee loss coefficients are defined in terms of flow and area ratios.

Pressure Equations for pipe (riser or manifold)

The pressure change equation for a pipe is given by the well known formulae [Miller(1978)]

$$\begin{aligned}\Delta p &= K d Q^2/2A^2 \\ &= (fL/D) d Q^2/2A^2\end{aligned}\quad (3.10)$$

The friction factor f is given by eqns (3.6) and (3.7) for laminar and turbulent flow respectively. L is the length of the pipe.

Pressure Equation for a Tee Junction

Following the definition of loss coefficient at a tee junction given in Sec. 3.1, the pressure change equations are given below. The same nomenclature follows.

Dividing Tee :

Throughflow

$$\begin{aligned}p_3 - p_2 &= d U_2^2/2 - d U_3^2/2 + K_{32} d U_3^2/2 \\ &= d Q_2^2/2A_2^2 - d Q_3^2/2A_3^2 + K_{32} d Q_3^2/2A_3^2\end{aligned}\quad (3.11)$$

Branch flow

$$\begin{aligned}
 p_3 - p_1 &= d U_1^2/2 - d U_3^2/2 + K_{31} d U_3^2/2 \\
 &= d Q_1^2/2A_1^2 - d Q_3^2/2A_3^2 + K_{31} d Q_3^2/2A_3^2 \quad (3.12)
 \end{aligned}$$

Combining Tee :

Throughflow

$$\begin{aligned}
 p_2 - p_3 &= d U_3^2/2 - d U_2^2/2 + K_{23} d U_3^2/2 \\
 &= d Q_3^2/2A_3^2 - d Q_2^2/2A_2^2 + K_{23} d Q_3^2/2A_3^2 \quad (3.13)
 \end{aligned}$$

Branch flow

$$\begin{aligned}
 p_1 - p_3 &= d U_3^2/2 - d U_1^2/2 + K_{13} d U_3^2/2 \\
 &= d Q_3^2/2A_3^2 - d Q_1^2/2A_1^2 + K_{13} d Q_3^2/2A_3^2 \quad (3.14)
 \end{aligned}$$

Eqns 3.10 - 3.14 form the basis of network pressure equations required to estimate the flow distribution in a solar collector array.

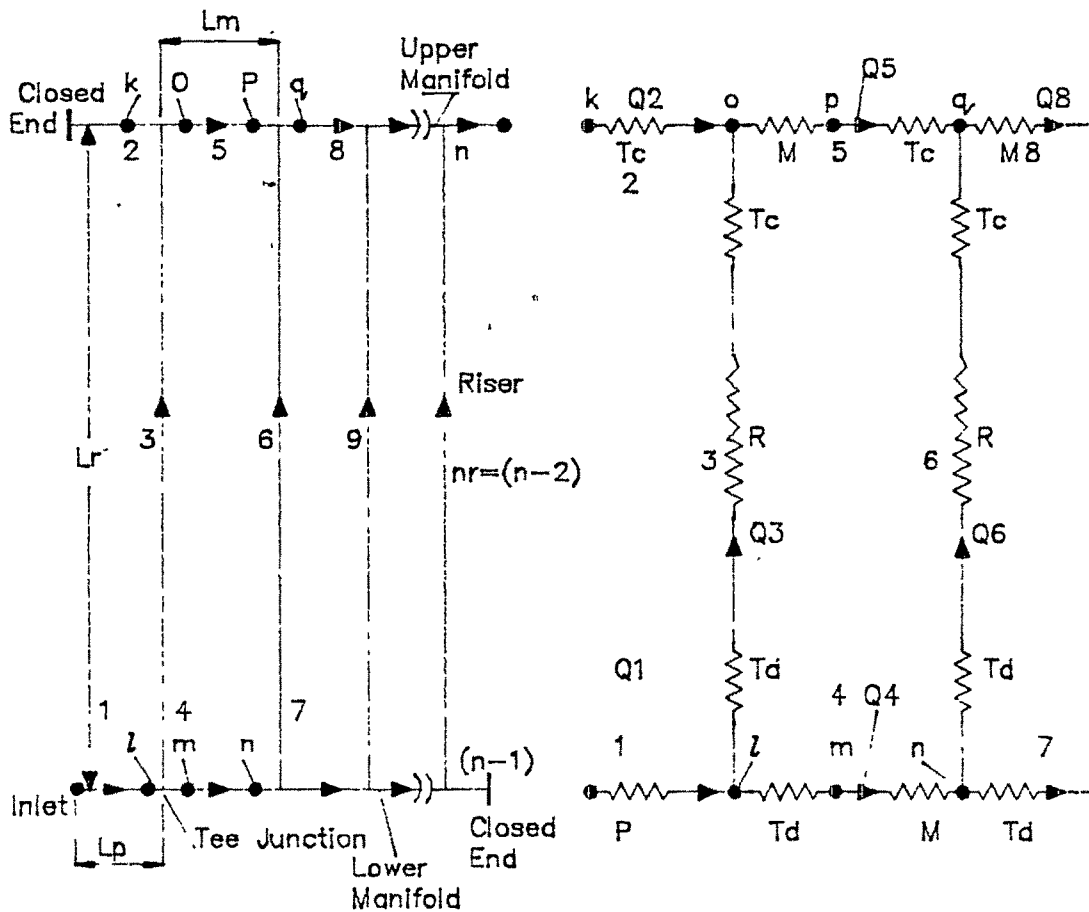
3.4 Network Pressure Equation for Asymmetric Flow

The solar collector with an internal manifold is shown in Fig. 1.1 (c). It can be modelled by a resistive network similar to electrical circuits. The resistive element represents the component in the pipe network which causes pressure change. These are essentially frictional losses in the riser and manifold, and the pressure loss or gain at the tee junctions where the riser meets the manifold.

Fig. 3.5 shows the collector hydraulic network and also the equivalent resistive network. The numbering of the hydraulic and the resistive network is done to facilitate computer modelling. It is seen from the resistive network that it has repetitive mesh which simplifies modelling and the solution of the network. It is therefore sufficient to write the equations for one close loop mesh, that is 3-4-6-5. The other meshes will have the same form.

The equations written for the branch represent the pressure change in the branch as shown in the resistive network of Fig. 3.5. In the total equations for the collector network, the potential head term will cancel out and thus not shown.

Considering mesh 3-4-6-5, the branch pressure equations are as follows :



Resistances

R: Riser, Frictional Loss Including Entrance Effect

M: Manifold, Frictional Loss Between Two 'T' Junctions

Tc: Combining 'T'; (13) and (23) Follows Nomenclature of Fig. 3.1

Td: Dividing 'T'; (31) and (32) Follows Nomenclature of Fig. 3.1

P: Inlet/Outlet Pipe

Fig. 3.5 Collector Hydraulic and Equivalent Resistance Network for Asymmetric Flow

$$p_b(3) = p_1 - p_o$$

= pressure change at dividing tee + pressure change in riser
due to friction + pressure change at combining tee

or

$$p_b(3) = d/2[(Q_3^2/A_3^2 - Q_1^2/A_1^2) + K_d(3,1)Q_1^2/A_1^2] \\ + f_3L_3/D_3 \quad d/2.Q_3^2/A_3^2 \\ + d/2[(Q_5^2/A_5^2 - Q_3^2/A_1^2) + K_c(3,5)Q_5^2/A_5^2] \quad (3.15)$$

or

$$p_b(3) = d/2.Q_1^2/A_1^2[K_d(3,1) - 1] + d/2.Q_3^2/A_3^2(f_3L_3/D_3) \\ + d/2.Q_5^2/A_5^2[K_c(3,5) + 1] \quad (3.16)$$

Since only two types of pipes are considered, i.e. riser and manifold, it will be easier to change the subscripts to riser and manifold. Thus, eqn 3.16 can be rewritten as

$$p_b(3) = d/2.Q_1^2/A_m^2[K_d(3,1) - 1] + d/2.Q_3^2/A_r^2(f_rL_r/D_r) \\ + d/2.Q_5^2/A_m^2[K_c(3,5) + 1] \quad (3.17)$$

where the subscripts *m* and *r* refer to manifold and riser respectively. It may be noted that the nomenclature of tee loss

coefficients has been slightly modified to avoid confusion with the branch numbering. Thus, $K_d(3,1)$ stands for dividing tee pertaining to flows in branches 3 and 1. While evaluating $K_d(3,1)$ from eqn 3.2 the corresponding flow rates are considered for computing the flow ratio, q . The same applies for $K_c(3,5)$, where the subscript c refers to combining tee.

On similar lines we get,

$$p_b(4) = d/2 \cdot Q_4^2 / A_m^2 [f_m L_m / D_m + 1] + d/2 \cdot Q_1^2 / A_m^2 [K_d(4,1) - 1] \quad (3.18)$$

$$p_b(5) = d/2 \cdot Q_5^2 / A_m^2 [f_m L_m / D_m - 1] + d/2 \cdot Q_8^2 / A_m^2 [K_c(5,8) + 1] \quad (3.19)$$

$$p_b(6) = d/2 \cdot Q_4^2 / A_m^2 [K_d(6,4) - 1] + d/2 \cdot Q_8^2 / A_r^2 (f_r L_r / D_r)$$

$$+ d/2 \cdot Q_4^2 / A_m^2 [K_c(6,8) + 1] \quad (3.20)$$

In general, the network pressure equations for asymmetric flow can be written as :

Riser

$$\begin{aligned}
 p_b(i) = & \frac{d}{2} \cdot \frac{Q_{i-2}^2}{A_m^2} [K_d(i, i-2) - 1] + \frac{d}{2} \cdot \frac{Q_i^2}{A_r^2} (f_r L_r / D_r) \\
 & + \frac{d}{2} \cdot \frac{Q_{i+2}^2}{A_m^2} [K_c(i, i+2) + 1] \qquad (3.21)
 \end{aligned}$$

Eqn 3.21 applies for $i = 3, 6, 9, \dots, (n-2)$

Lower manifold

$$p_b(i) = \frac{d}{2} \cdot \frac{Q_i^2}{A_m^2} [f_m L_m / D_m + 1] + \frac{d}{2} \cdot \frac{Q_{i-3}^2}{A_m^2} [K_d(i, i-3) - 1] \qquad (3.22)$$

$$i = 4, 7, 10, \dots, (n-2)$$

Upper manifold

$$p_b(i) = \frac{d}{2} \cdot \frac{Q_i^2}{A_m^2} [f_m L_m / D_m - 1] + \frac{d}{2} \cdot \frac{Q_{i+3}^2}{A_m^2} [K_c(i, i+3) + 1] \qquad (3.23)$$

$$i = 2, 5, 8, \dots, n$$

where, n = total no. of branches

$$= 3n_r + 2$$

n_r = no. of risers in a collector

In evaluating the tee loss coefficients $K_a(i,j)$ and $K_c(i,j)$ in eqns 3.21 - 3.23, the flow ratio q , as defined in Sec. 3.1 and eqns 3.2 - 3.5, is always computed as :

Riser

$$q = Q_i/Q_j$$

or $q = Q_i/Q_{i-2}$ for dividing flow,

$$= Q_i/Q_{i+2} \text{ for combining flow} \quad (3.24)$$

Lower manifold

$$q = Q_{i-1}/Q_j = Q_{i-1}/Q_{i-3} \quad (3.25)$$

Upper manifold

$$q = Q_{i+1}/Q_j = Q_{i+1}/Q_{i+3} \quad (3.26)$$

since the flow ratio is always defined as the ratio of branch to the total flow.

The area ratio is always

$$a = A_r/A_m \quad (3.27)$$

For asymmetric flow, $Q_2 = Q_{n-1} = 0$, since branches 2 and $n-1$ are the closed ends.

The pressure change at the inlet and outlet pipes is given by

$$p_b(i) = d/2 \cdot Q_1^2 / A_m^2 (f_p L_p / D_p) \quad (3.28)$$

where, $i = 1$ or n

L_p = length of inlet/outlet pipe, m

D_p = diameter of inlet/outlet pipe, m

3.5 Network Pressure equation for Symmetric Flow

Fig. 3.6 shows the collector hydraulic network for symmetric flow. Considering the mesh 3-4-6-5 we get

$$\begin{aligned}
 p_b(3) = & \quad d/2[(Q_3^2/Ar^2 - Q_1^2/Am^2) + K_d(3,1)Q_1^2/Am^2] \\
 & + d/2.Q_3^2/Ar^2(frL_r/Dr) \\
 & + d/2[(Q_2^2/Am^2 - Q_3^2/Ar^2) + K_c(3,2)Q_2^2/Am^2] \quad (3.29)
 \end{aligned}$$

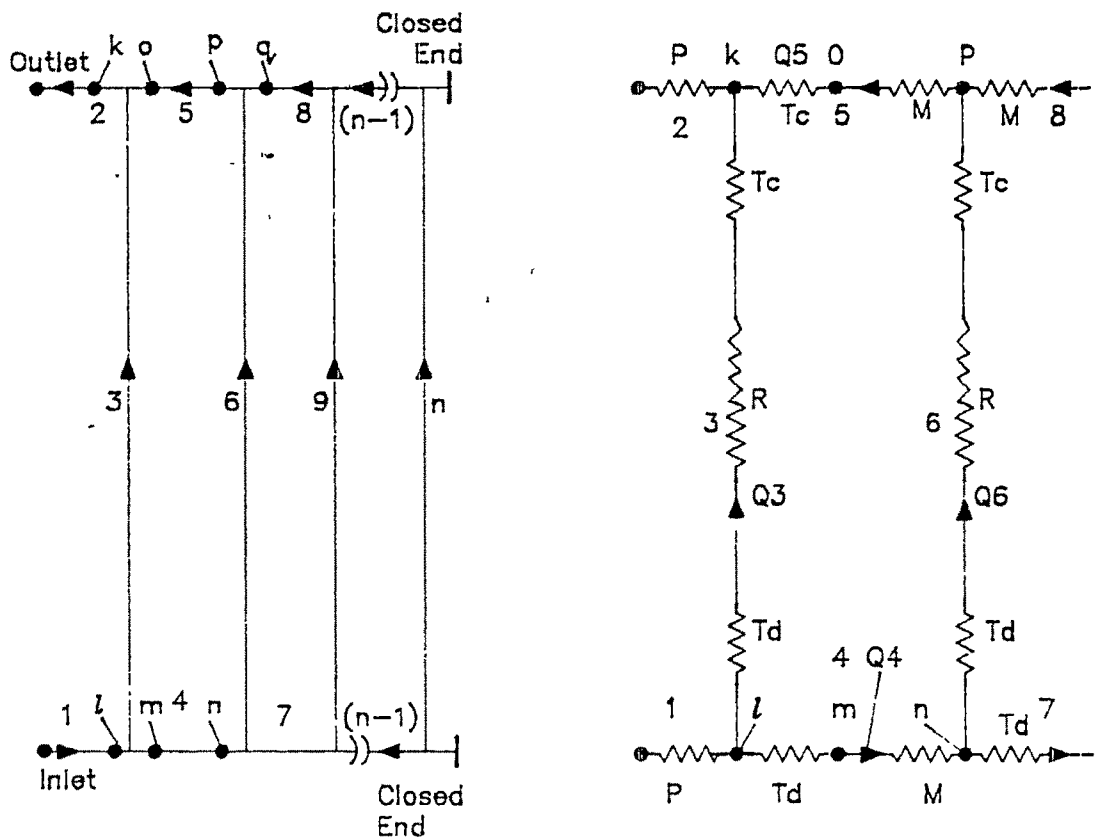
or

$$\begin{aligned}
 p_b(3) = & \quad d/2.Q_1^2/Am^2[K_d(3,1) - 1] + d/2.Q_3^2/Ar^2(frL_r/Dr) \\
 & + d/2.Q_2^2/Am^2[K_c(3,2) + 1] \quad (3.30)
 \end{aligned}$$

$$\begin{aligned}
 p_b(4) = & \quad d/2.Q_4^2/Am^2(fmL_m/D_m + 1) + d/2.Q_1^2/Am^2[K_d(4,1) - 1] \\
 & \dots\dots(3.31)
 \end{aligned}$$

$$\begin{aligned}
 p_b(5) = & \quad d/2.Q_5^2/Am^2(fmL_m/D_m - 1) + d/2.Q_2^2/Am^2[K_c(5,2) + 1] \\
 & \dots\dots(3.32)
 \end{aligned}$$

$$\begin{aligned}
 p_b(6) = & \quad d/2.Q_4^2/Am^2[K_d(6,4) - 1] + d/2.Q_8^2/Ar^2(frL_r/Dr) \\
 & + d/2.Q_5^2/Am^2[K_c(6,5) + 1] \quad (3.33)
 \end{aligned}$$



Resistances

- R: Riser, Frictional loss Including Entrance Effect
- M: Manifold, Frictional Loss Between Two 'T' Junctions
- Tc: Combining 'T'; (13) and (23) Follows Nomenclature of Fig. 3.1
- Td: Dividing 'T'; (31) and (32) Follows Nomenclature of Fig. 3.1
- P: Inlet/Outlet Pipe

Fig. 3.6 Collector Hydraulic Network and Equivalent Resistance Network for Symmetric Follow

In general, the network pressure equations for symmetric flow can be written as :

Riser

$$\begin{aligned}
 p_b(i) = & d/2 \cdot Q_{i-2}^2 / A_m^2 [K_d(i, i-2) - 1] + d/2 \cdot Q_i^2 / A_r^2 (f_r L_r / D_r) \\
 & + d/2 \cdot Q_{i-1}^2 / A_m^2 [K_c(i, i-1) + 1]
 \end{aligned} \tag{3.34}$$

$$i = 3, 6, 9 \dots n$$

Lower manifold

$$p_b(i) = d/2 \cdot Q_i^2 / A_m^2 [(f_m L_m / D_m) + 1] + d/2 \cdot Q_{i-3}^2 / A_m^2 [K_d(i, i-3) - 1] \tag{3.35}$$

$$i = 1, 4, 7 \dots (n-2)$$

Upper manifold

$$p_b(i) = d/2 \cdot Q_i^2 / A_m^2 [(f_m L_m / D_m) - 1] + d/2 \cdot Q_{i-3}^2 / A_m^2 [K_c(i, i-3) + 1] \tag{3.36}$$

$$i = 2, 5, 8 \dots (n-1)$$

where n = total no. of risers

$$= 3n_r$$

n_r = no. of risers

In evaluating the tee loss coefficients $K_d(i,j)$ and $K_c(i,j)$, the flow ratio q is always computed as :

Riser

$$\begin{aligned}
 q &= Q_i/Q_j \\
 &= Q_i/Q_{i-2} \text{ for dividing flow} \\
 &= Q_1/Q_{i-1} \text{ for combining flow}
 \end{aligned}
 \tag{3.37}$$

Lower manifold

$$q = Q_{i-1}/Q_j = Q_{i-1}/Q_{i-3} \tag{3.38}$$

Upper manifold

$$q = Q_{i-2}/Q_j = Q_{i-2}/Q_{i-3} \tag{3.39}$$

The area ratio is similarly defined by eqn 3.27. The pressure change at the inlet/outlet pipe is given by

$$p_b(i) = d/2 \cdot Q_i^2 / A_m^2 (f_p L_p / D_p) \tag{3.40}$$

$$i = 1 \text{ or } 2$$

3.6 Solution of Solar Collector Hydraulic Network

The solution of a pipe network is defined as the determination of the flows in the pipes and the pressures at the junctions given the structure of the network, physical dimension, the external flows and the physical properties of the flowing fluid. Most of the methods available are due to Hardy Cross (1936) which is essentially a relaxation method. The Hardy Cross method is based on Kirchoff's laws :

1. The algebraic sum of flows at any pipe junction is zero.
2. The algebraic sum of the pressure drops around any closed loop (mesh) of the network is zero.

A relationship between pressure drop and flow is needed to solve the network. This was derived in Sec. 3.4 and 3.5 for the asymmetric and symmetric flow networks respectively.

The above two laws lead to two iteration schemes. In the first scheme, the method of balancing heads, a flow distribution which satisfies the first law is assumed and is subjected to correction mesh by mesh until the requirements of the second law are satisfied. The second method, the method of balancing flows, starts from a pressure distribution which satisfies the second law and which is iterated until the first law is satisfied.

The algorithm developed subsequently, the latest of which is due to Daniel (1966), used essentially the same technique with slight modifications. The main disadvantage of the Hardy Cross technique is that it requires selection of a set of meshes for the network. For a large network this is not a trivial task since there is no unique set of meshes and furthermore the rate of convergence of the solution depends upon the selection made. In addition, an initial distribution of flow (or pressures) which satisfies one of Kirchoff's laws must be calculated. This could be quite complex.

To overcome these, Gay and Middleton (1971) developed a diakoptics technique. The technique involves transforming a network into an intermediate network whose solution can be found and the transforming this solution into the solutions of the given network. This is essential since in the Hardy Cross method the rate of convergence depends strongly upon selection of mesh. Daniel (1977) developed a computer program to find a set of basic meshes given a tree of the network. However, this procedure transforms the problem of mesh selection into the problem of tree selection. Daniel found this was computationally prohibitive. In this respect, the diakoptics method is superior.

Bending and Hutchinson (1973) developed another algorithm, called linearisation technique, which is simpler in concept compared to the previous methods discussed above and requires less computation time.

3.6.1 Selection of Network Algorithm

The techniques developed by Gay and Middleton (1971), and Bending and Hutchinson (1973) are basically for very large pipe networks which are difficult to solve by simpler techniques. The techniques involve matrix representation and its solution is strongly dependent upon the network matrix correlating the flow and pressure in the branches. The diakoptics essentially simplifies the matrix amenable to solution. So is the case with the linearisation technique.

For the present work a simpler algorithm will be adequate since the closed loop meshes are identical. That is, the closed loop between the two risers is repetitive, as shown in Fig. 3.5 by mesh 3-4-6-5. Thus no tree selection or mesh selection is required to assure convergence. It is also not necessary to resort to matrix transformation and inversion needed in diakoptics and linearisation methods. For these reasons, Daniel's algorithm which is an advanced version of Hardy Cross technique is employed.

3.6.2 Daniel's Algorithm for Solar Collector

The relationship between pressure drop and flow in a branch i of a network can be expressed as

$$p_b(i) = R_i Q_i^2 \quad (3.41)$$

The resistance factor R_i is the resistance of the branch i and can be derived easily from the pressure change eqns 3.21-3.23 and 3.34-3.36 described in Secs. 3.4 and 3.5.

A steady state solution is found when the algebraic sum of the pressure drops round all the meshes are zero. Thus, for a single mesh

$$\sum R_i Q_i^2 = 0 \quad (3.42)$$

While carrying out computation, eqn 3.42 is satisfied for all meshes if the amount by which the pressure drop is out of balance is arbitrarily small.

The Hardy Cross method assumes that each branch in the network is assigned a flow such that Kirchoff's first law is obeyed, that is

$$\sum Q_i = 0 \quad (3.43)$$

This is called initial solution and it is not necessary that at this stage eqn 3.42 is satisfied. Generally, the initial estimate of flow will result in eqn 3.42 being out of balance. This will be termed as a mesh current. The object is to successively improve the initial estimate until a sufficiently accurate solution is achieved. This is done by obtaining the Hardy Cross correction factor caused by the inaccuracy of the initial estimate of flows for each basic mesh. The correction factor is then applied to the flows in the branches forming the mesh. The improvement to the current best estimate (n^{th} iterate) may be carried out by

$$Q_i^{n+1} = Q_i^n + q_m^n \quad (3.44)$$

q_m is the Hardy-Cross correction factor, the sign of which is dependent upon the accuracy of the initial branch flow.

Rewriting eqn 3.44 gives

$$Q_i^{n+1} = Q_i^n + C_{m,k} q_m^n \quad (3.45)$$

where $C_{m,k}$ are the the elements of circuit matrix shown in Fig. 3.7 and is described below. The correction factor q_m is given by

$$q_m = \frac{- \sum C_{m,k} \text{sign } Q_i^n R_i (Q_i^n)^2}{\sum 2 | C_{m,k} R_i Q_i^n |} \quad (3.46)$$

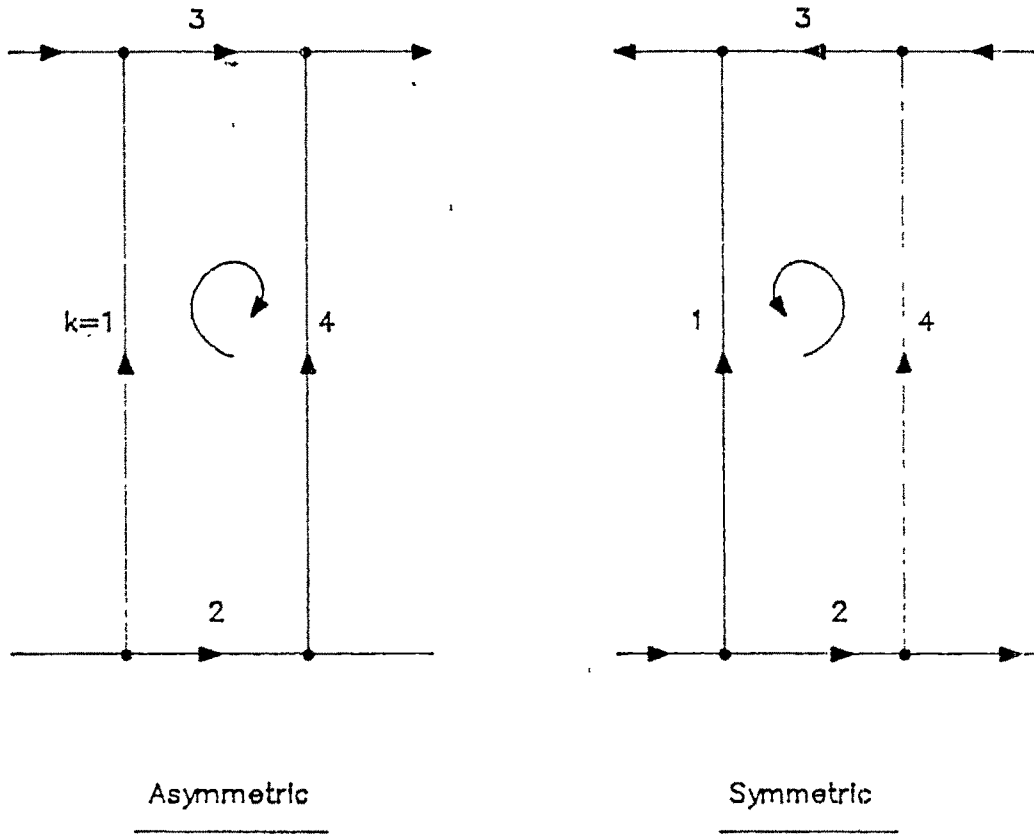
here $k=4$

3.6.3 Circuit Matrix

Fig. 3.7 shows the circuit matrices for asymmetric and symmetric flow. The circuit matrix is a logical matrix having value of 1 or -1. The assignment of value is dependent upon the arbitrary mesh flow chosen. In Fig. 3.7 the mesh flow is clockwise for asymmetric flow while it is anti-clockwise for symmetric flow. The subscript m corresponds to mesh number in the network while k refers to the branches in the mesh. The value assignment is given below :

$C_{m,k} = 1$, if the flow in branch i in the m^{th} mesh coincides with the mesh flow.

$C_{m,k} = -1$, if the flow in branch i in the m^{th} mesh is opposite to the mesh flow.



<u>C_{m,k}</u>	<u>Value</u>
C _{m,1}	1
C _{m,2}	-1
C _{m,3}	1
C _{m,4}	-1

<u>C_{m,k}</u>	<u>Value</u>
C _{m,1}	-1
C _{m,2}	1
C _{m,3}	1
C _{m,4}	1

Fig. 3.7 Circuit Matrices for Asymmetric and Symmetric Flow

3.7 Flow Reversals

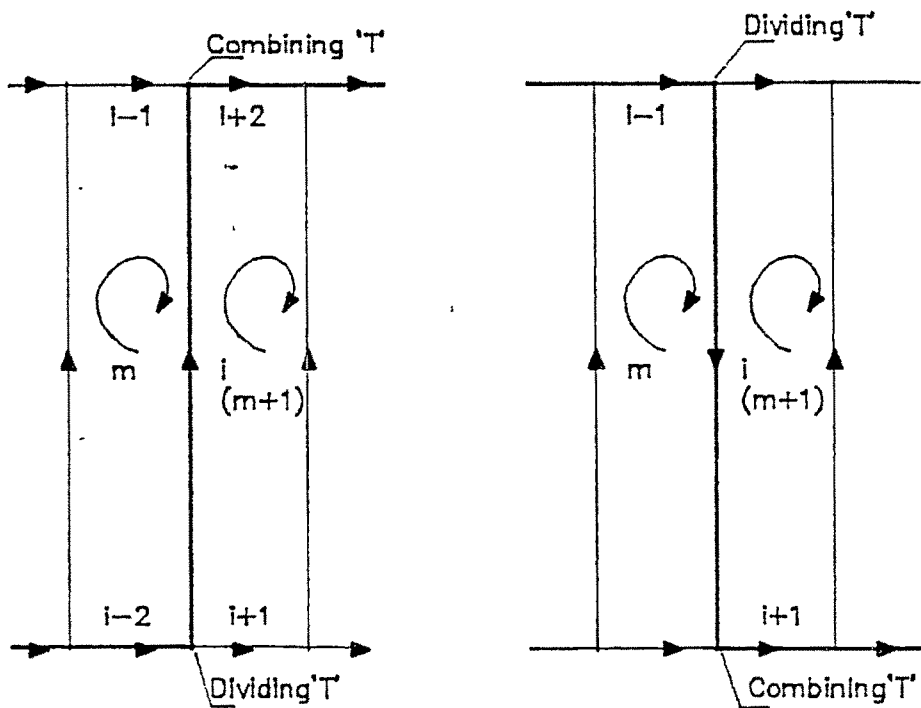
Flow can reverse in a riser due to unfavorable collector geometry, for example, high resistance of pipe interconnecting two collector modules or in case the riser diameter is higher than that of the manifold as observed by McPhedran (1983). In case of later, the manifold offers more resistance than the risers. It can also occur during iterations during balancing with orifices, which again is due to high resistance in the interconnecting pipe. The flow reversal can be taken care of easily by reformulating the resistance network. Essentially, the dividing tee will become a combining tee and vice-versa.

Fig 3.8 shows a portion of a network illustrating flow reversal in the i th riser. The necessary modifications in the network definitions are indicated. Also the corresponding changes in the resistance network are also illustrated in Fig. 3.9 for asymmetric flow.

Flow reversal in two adjacent risers and in alternate risers are also considered and incorporated in the model as described above. The treatise for symmetric flow remains the same.

3.8 Effect of Temperature

The network equations derived in Sec.3.4 and 3.5 were for isothermal fluid. In an actual solar collector this will not be the



(a) Normal Flow in Branch i

(b) Reverse Flow in Branch i

Flow Ratio

$q = Q_i / Q_{i-2}$, Dividing Flow

$q = Q_i / Q_{i+2}$, Combining Flow

Circuit Matrix

$C_{m,4} = -1$

$C_{m+1,1} = 1$

Flow Ratio

$q = |Q_i| / |Q_{i-1}|$

$q = |Q_i| / |Q_{i+1}|$

Circuit Matrix

$C_{m,4} = 1$

$C_{m+1,1} = -1$

Fig. 3.8 Modifications in the Network during Flow Reversal in flow ratio and circuit Matrix in Asymmetric Flow

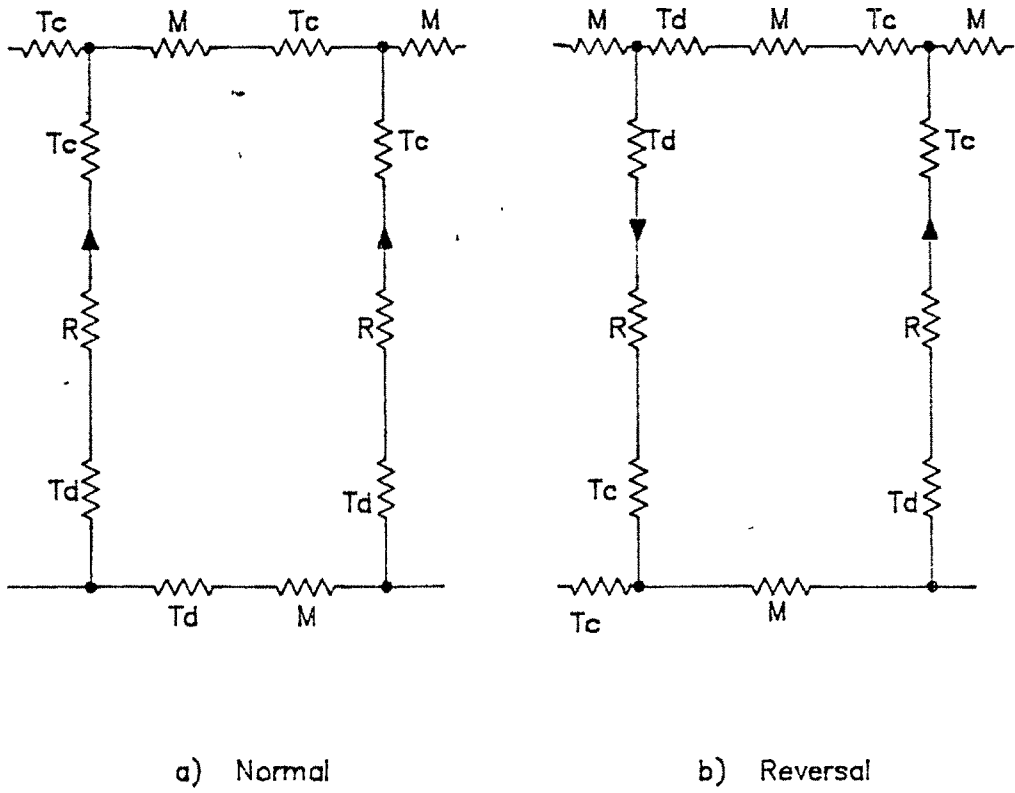


Fig.3.9 Modification in resistance Network
Due to Flow Reversal in Asymmetric Flow

case since the fluid temperature increases across the riser. The temperature difference which can affect the flow behaviour can be of two types.

Firstly, the temperature difference across the riser due to temperature gained by the flowing fluid. This affects the density and viscosity, which in turn affect parameter like friction factor and thus the pressure drop. Secondly, difference in the fluid temperatures between parallel risers due to maldistribution which induces a thermosiphon head due to density difference.

In a solar collector, the temperature rise per pass across the riser is typically 10° - 20° C depending upon the flow rate, collector characteristics and solar intensity. For solar collector with selective coating and one cover, typical of present day collector, the temperature rise will be computed as follows.

The Hottel-Whillier-Bliss equation can be used to compute temperature rise [Duffie(1974)] :

$$dT = \frac{FR [I.(ta) - UL(Ti - Ta)]}{G C_p} \quad (3.47)$$

where FR = collector heat removal factor, dimensionless

I = solar radiation, W m⁻²

(ta)= transmittance-absorptance product

U_L = overall collector loss coefficient, $W m^{-2}K^{-1}$

T_i = fluid inlet temperature, K

T_a = ambient temperature, K

G = collector flow rate per unit area, $kg s^{-1}m^{-2}$

C_p = fluid specific heat, $J kg^{-1}K$

Typically, one cover selective collector and operating conditions will have the following values :

$(\tau\alpha) = 0.84$

$U_L = 4.0 \quad W m^{-2}K^{-1}$

$G = 0.0050 - 0.0075 \quad kg s^{-1}m^{-2}$

$C_p = 4190 \quad J kg^{-1}k^{-1}$

$I = 300 - 1000 \quad W m^{-2}$

$T_i = 25 - 40 \quad ^\circ C$

$T_a = 25 - 40 \quad ^\circ C$

For estimating the effect of temperature difference across the riser, all the conditions chosen below will result in daytime average temperature rise :

$G = 0.0075, I = 800, T_i = 30 \text{ } ^\circ C, T_a = 25 \text{ } ^\circ C.$

F_R can be estimated from the following [Duffie(1974)] :

$$F_R = \frac{G C_p}{U_L} [1 - \exp(- F' U_L / G C_p)] \quad (3.48)$$

where F' = collector efficiency factor, typically equals 0.98 for 1 cover selective collector.

Thus, $F_R = 0.92$ for $G = 0.0075 \text{ kgs}^{-1}\text{m}^{-2}$.

Using the above values, the temperature rise across the riser is 18.5°C . Considering the changes in density and viscosity at inlet and outlet, the friction factor differs only by 2 - 3 %. The change due to increasing the inlet temperature for the same temperature rise also is not more than 3 %. The effect of temperature rise across the riser on the pressure drop computation can thus be neglected.

The temperature effect will be even insignificant when the collector array is designed for nearly uniform flow distribution. In this case, the temperature rise in all the risers being practically the same, the change in the riser pressure drop will be almost identical. This, effectively, implies that the riser characteristics being almost the same, the overall effect on the flow distribution will be negligible.

The temperature difference in the parallel risers will occur due to maldistribution. This temperature difference will create a

thermosiphon head. It was shown by McPhedran (1983) that this could be quite small relative to the riser pressure drop. This is true for all cases where the riser pressure drop is controlling. Further, it may be argued that for an array with low flow maldistribution, the thermosiphon head will be small. And for a forced circulation system this head will be small.

3.9 Collector Array Efficiency

Knowing the flow distribution in terms of actual flow rates in the risers, it is possible to estimate the collector array efficiency. Smirnov (1981) and Cawphob (1981) derived a simple expression which can be utilised to estimate the effect of flow maldistribution on the collector efficiency. Cawphob's expression was used by Jiang and Mao (1985) discussed in Chapter 2 and was found useful in describing the experimentally determined array efficiency.

The collector array efficiency will then quantitatively determine the effect of flow maldistribution. This will allow a designer to determine the number collectors which can be placed in parallel for a given collector geometry and flow rate within specified reduction allowable in the collector array efficiency.

Both Smirnov (1981) and Cawphob (1981) employed the basic collector heat transfer equation given by eqns 3.48. These

equations apply to a collector or an individual fin-riser. While the above authors had considered a collector as a unit for analysing the flow distribution, in the present work an individual fin-riser assembly is considered. Majority of the present day commercial solar collectors have individual fin-riser placed together to form a collector. The individual fin-risers are normally not joined together thermally. In certain designs they are overlapping without good thermal contact.

In the following, the collector array efficiency is derived for solar collector array comprising of several collectors having a number of independent fin-riser. Eqn 3.47 is rewritten to give the useful heat gained by the i^{th} fin riser

$$Q_{u^i} = FR^i [I (t_a) - U_L (T_i - T_a)] \quad (3.49)$$

The heat removal factor, FR , is defined by eqn 3.48.

Assuming that the inlet fluid temperature T_i and the overall loss coefficient U_L are identical for all the risers, and summing up for all the risers, the overall useful heat gained by the array is given by

$$\sum Q_{u^i} = [I (t_a) - U_L (T_i - T_a)] \sum FR^i \quad (3.50)$$

When the flow is uniformly distributed, the useful heat gained by the fin-riser is

$$Q_u^* = FR^* [I (t_a) - U_L (T_i - T_a)] \quad (3.51)$$

The total useful heat gained by the array will be nrQ_u^* , since flow is uniform in each riser.

The collector array efficiency is simply given by

$$\begin{aligned} \text{ceff}_s &= \sum Q_{u^i} / (nr Q_u^*) \\ &= \sum FR^i / (nr FR^*) \end{aligned} \quad (3.52)$$

Eqn 3.48 can be rewritten as

$$FR = F' x [1 - \exp(-1/x)] \quad (3.53)$$

$$\text{where } x = G C_p / U_L F' \quad (3.54)$$

Following Smirnov (1981) by expanding $FR(x_i)$ into series of power of $(x_i - x^*)$ and retaining second order terms only, an approximation of ceff_s is obtained.

$$\text{ceff}_s \approx 1 - \frac{1}{2(x^*)^4 [\exp(1/x^*) - 1]} \sum (x_i - x^*) \quad (3.55)$$

The above can be simplified to

$$\text{ceff}_s \approx 1 - \frac{1}{2(x^*)^2 [\exp(1/x^*) - 1]} \sum_{nr} (x_i/x^* - 1) \quad (3.56)$$

$$\text{Since } \frac{x_i}{x^*} = \frac{G_i}{G^*} = \frac{Q_i}{Q^*} \quad (3.57)$$

the summation term in eqn 3.60 can be replaced by

$$\frac{1}{nr} \sum_{nr} \left[\frac{Q_i}{Q^*} - 1 \right] \quad (3.58)$$

Q_i and Q^* are the i^{th} riser flow rate and the riser flow rate with uniform flow in the array, respectively. The quantity Q_i for all the risers are known from the solution of the network.

Eqs 3.56 and 3.58 are used to estimate the collector array efficiency with respect to an array with uniform flow. In the present work the summation term of eqn 3.58 is considered equivalent to the non-uniformity factor and is used in Chapter 6.

Application of Non-uniformity Factors

The collector array efficiency derived above will not be applicable to collectors having fin-riser in good thermal contact,

since there will be redistribution of temperature in the adjacent fin-risers. This is not serious since normally only 8 to 10 risers are placed in a collector. Smirnov's collector array efficiency will therefore serve as an upper limit.

3.10 Computer Model Flow Chart

The flow chart given in Fig. 3.10 describes the procedure for solving the hydraulic network.

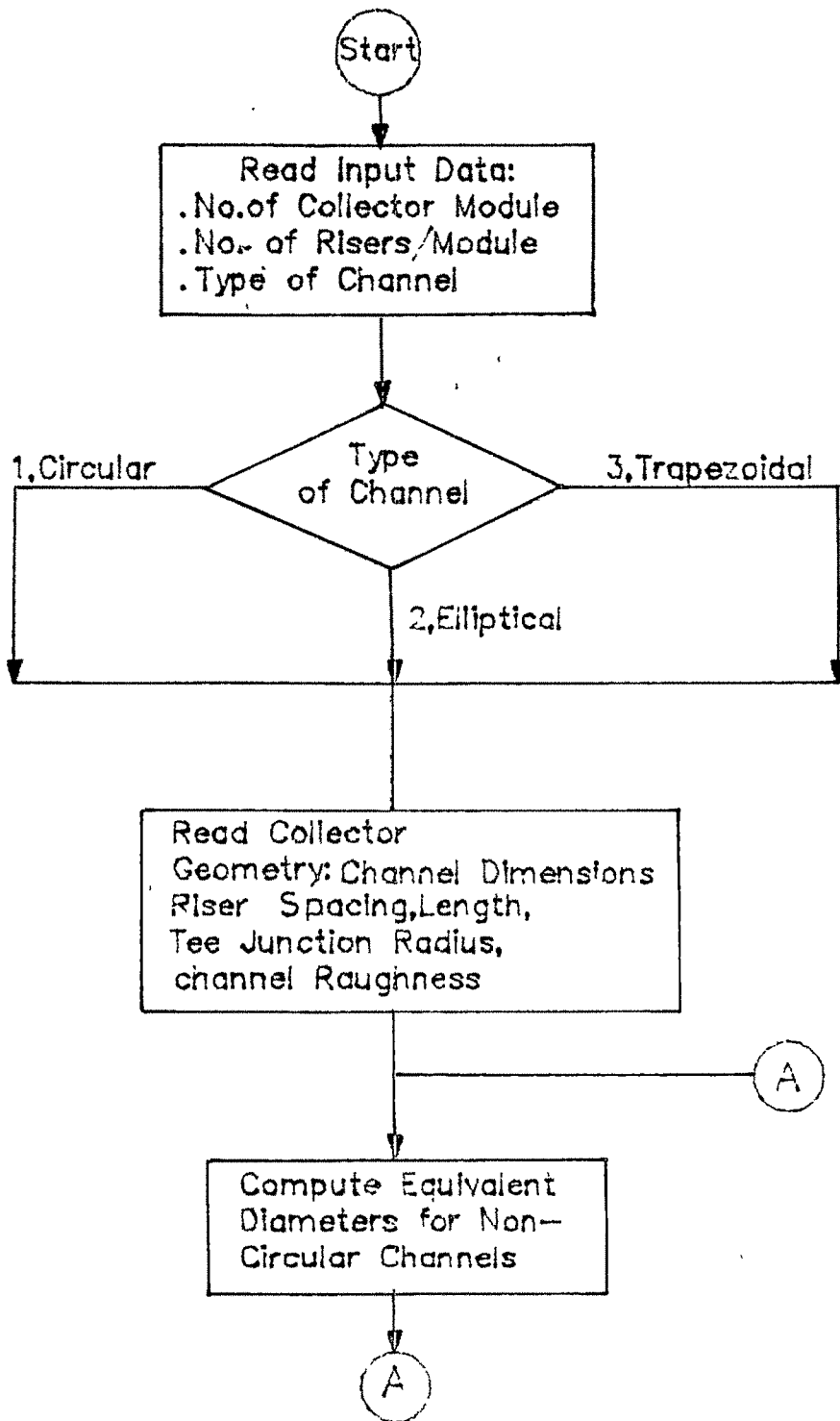


Fig. 3.10 Flow Chart for Solving Collector Hydraulic Network (Asymmetric and Symmetric)

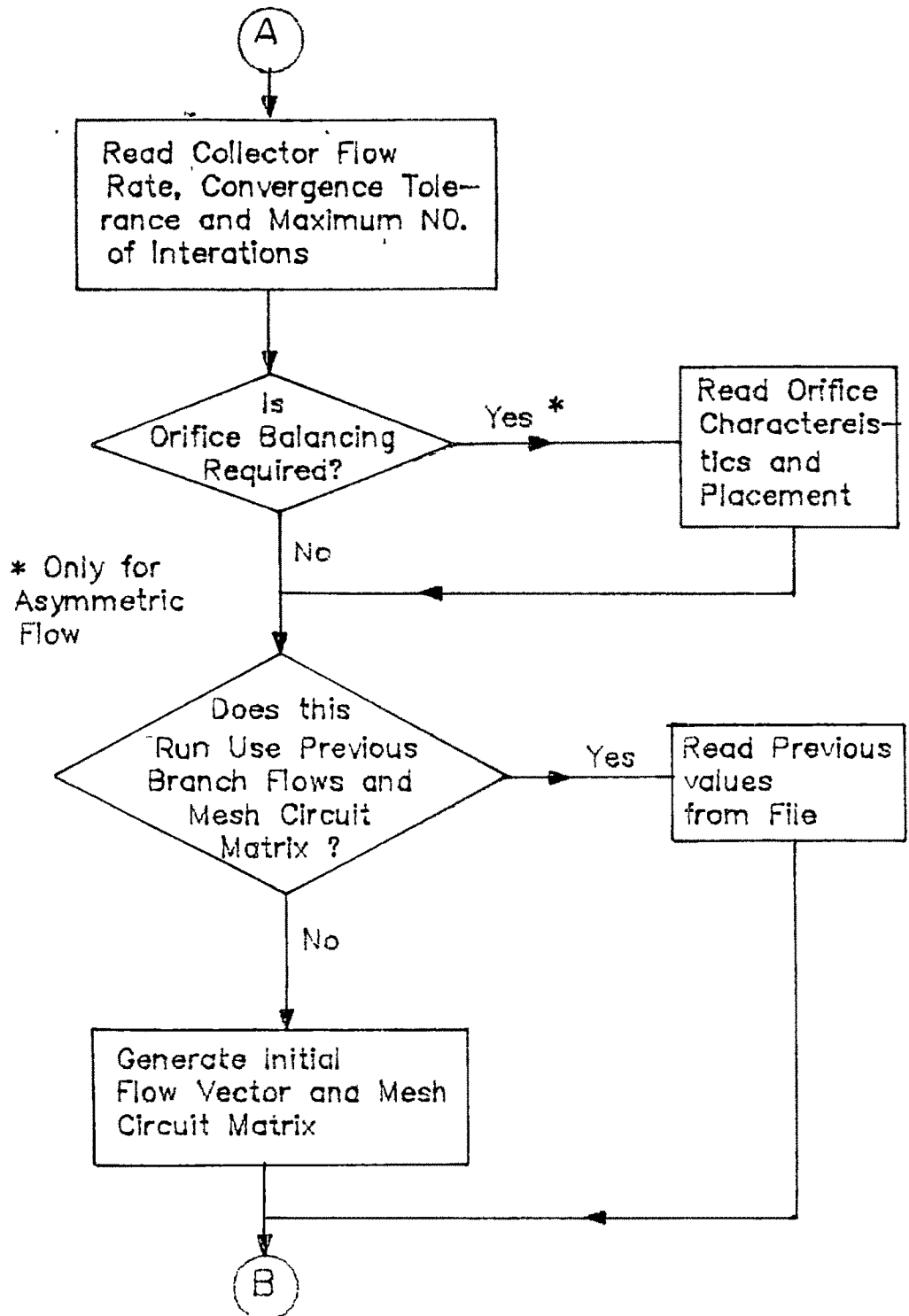


Fig. 3.10 Cont'd

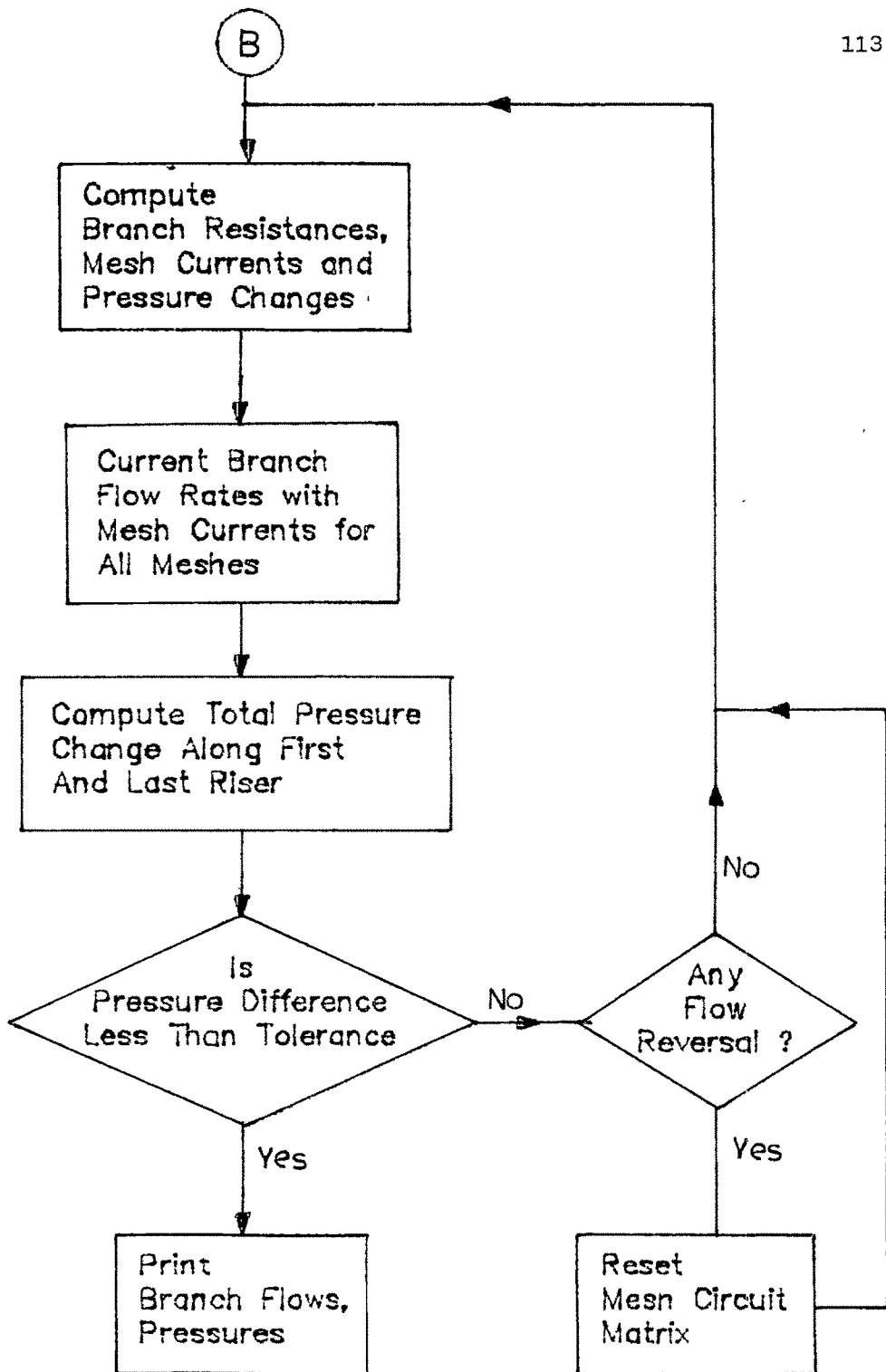


Fig. 3.10 Cont'd